(31) For a preliminary communication of this work see: Bloembergen, S.; Holden, D. A.; Hamer, G. K.; Bluhm, T. L.; Marchessault, R. H. *Polym. Prepr. (Am. Chem. Soc., Div. Polym. Chem.)* **1986**, *27*(2).
(32) Griffiths, P. R. *Chemical Infrared Fourier Transform Spectroscopy*; Wiley: New York, 1975.
(33) Doi, Y.; Kunioka, M.; Nakamura, Y.; Soga, K. *Macromolecules* **1986**, *19*, 1274.

Isodimorphism in Bacterial Poly(β-hydroxybutyrate-*co*-β-hydroxyvalerate)

Terry L. Bluhm, Gordon K. Hamer, and Robert H. Marchessault*

Xerox Research Centre of Canada, 2660 Speakman Drive, Mississauga, Ontario, Canada L5K 2L1

Colin A. Fyfe and Richard P. Veregin

Guelph–Waterloo Centre for Graduate Work in Chemistry, Department of Chemistry, University of Guelph, Guelph, Ontario, Canada N1G 2W1. *Received July 7, 1986*

ABSTRACT: Bacterial copolymers from *Alcaligenes eutrophus* containing β-hydroxybutyrate and β-hydroxyvalerate monomer units were characterized by X-ray diffraction, differential scanning calorimetry, solution NMR, and solid-state ^{13}C NMR. The copolyesters were shown to be statistically random and of high crystallinity (>60%) throughout a range of compositions varying from 0 to 47 mol % β-hydroxyvalerate units. A minimum in the melting point vs. composition curve was found at approximately 30 mol % β-hydroxyvalerate. Only two crystal forms were detected: the β-hydroxybutyrate crystalline phase on one side of the melting point minimum and the β-hydroxyvalerate crystalline phase on the other. Solid-state ^{13}C NMR spectra support the conclusion that the poly(β-hydroxybutyrate-*co*-β-hydroxyvalerate) system is isodimorphic with each crystalline phase accommodating the repeating unit of the other monomer as part of its organized structure.

Introduction

This study involves the characterization of optically active copolyesters (Figure 1) of β-hydroxybutyrate (HB) and β-hydroxyvalerate (HV) as well as the reference homopolyester, poly(β-hydroxybutyrate) (PHB). These materials have recently been introduced by Imperial Chemical Industries (ICI) as biotechnology products with thermoplastic properties.[1] This is the first time that PHB has been available in commercial quantities.

Recently some of us reported[2] on the physical properties of chiral PHB and poly(β-hydroxyvalerate) (PHV) derived from sewage sludge.[3] In that case, it was concluded that the isolated polymeric material was a physical mixture of the two homopolymers. In the present study, X-ray diffraction, differential scanning calorimetry, solution NMR, and solid-state ^{13}C NMR were used to characterize a series of P(HB-*co*-HV) samples, which had been obtained from homogeneous bacterial cultures by a patented procedure.[4] These copolyesters have a statistically random distribution of comonomer units and approximately the same high degree of crystallinity, while exhibiting a minimum in their melting point vs. composition curve. The phenomenon explaining this behavior is called isodimorphism.[5] In this paper data are presented to substantiate the hypothesis of P(HB-*co*-HV) isodimorphism.

Experimental Section

Materials. The PHB and P(HB-*co*-HV) samples used in this work were obtained from Dr. P. A. Holmes, ICI Agricultural Division, Billingham, UK. Similar materials are commercially available from ICI under the trade name Biopol. As received, the samples were semicrystalline powders that had been isolated from *Alcaligenes eutrophus* cultures and precipitated from chloroform solution by the addition of methanol.[4] The range of P(HB-*co*-HV) compositions, as measured by ^1H NMR spectroscopy,[6] was 0–47 mol % HV.

NMR Spectroscopy. Solution ^1H and ^{13}C NMR spectra were recorded on a Bruker WM-250 spectrometer operating at 250.13 MHz for ^1H and 62.9 MHz for ^{13}C. Samples were prepared in chloroform-*d* (10–20 mg/mL for ^1H, 40–50 mg/mL for ^{13}C) containing tetramethylsilane (Me_4Si, $\delta = 0$) as an internal chemical shift standard. Proton spectra were recorded at ambient temperature (23 °C) with a spectrum width of 2500 Hz, 32K data points, a 45° pulse (2 μs), and 16–128 transients. Proton-decoupled ^{13}C spectra were obtained at 32 °C with a 12500-Hz spectral width, 32K data points, a 45° pulse (12.5 μs), and typically 15000–30000 transients. The ^{13}C FID was zero-filled three times before Fourier transformation to provide adequate digital resolution (0.095 Hz/point) to accurately define the peak line shape. Resolution-enhanced spectra were obtained by a Lorentz–Gauss transformation of the FID[7] using a line broadening of −1 to −1.5 Hz and a Gaussian multiplication factor of 0.3–0.4. Peak areas were determined from unenhanced spectra by spectrometer integration and/or by curve fitting. The latter procedure utilized LINESIM,[8] an interactive Pascal program for the Bruker Aspect 2000 computer. A sum of Lorentzian lines of equal but variable line width was visually fit to the experimental bandshape by using the residual sum of squares as a goodness-of-fit criterion. Individual peak areas were calculated from the height and width values for the optimized fit.

Solid-state ^{13}C cross-polarization magic-angle-spinning (CP/MAS) NMR spectra were recorded at 22.6 MHz on a Bruker CXP-100 spectrometer using a home-built probe and room-temperature spinning apparatus. Measurements were made for as-received powder samples and films cast from chloroform solution. Stretched films were prepared by extension to break and annealed samples by heating at 20 °C below the melting point for 1 h after stretching. CP/MAS spectra were obtained with spin locking and decoupling fields of ~10 G and spinning rates of ~2.5 kHz. A 1-ms contact time and 1-s recycle delay were used, yielding semiquantitative results.[9] Chemical shifts were referenced to external hexamethyldisiloxane (by substitution) and converted to the Me_4Si scale by adding 2.1 ppm to the measured values.

Thermal Analysis. Thermal data were recorded on a Perkin-Elmer DSC-2C instrument previously calibrated with an indium standard. Samples were annealed by heating at 20 °C/min to within 20 °C of the melting point and then cooling at 20 °C/min to room temperature. DSC traces were recorded at 20, 10, and 5 °C/min; slower heating rates were not used to avoid thermal degradation of the polyester sample. Melting points were determined by extrapolation to zero heating rate. Where multiple endotherms were observed, the melting point from the higher temperature endotherm was taken as the true melting point.

0024-9297/86/2219-2871$01.50/0

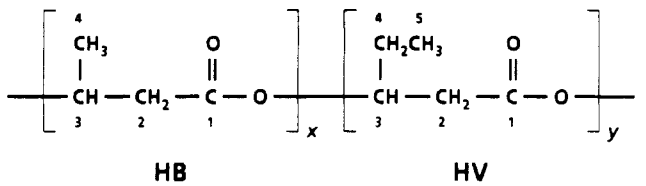

Figure 1. Schematic structure of poly(β-hydroxybutyrate-*co*-β-hydroxyvalerate).

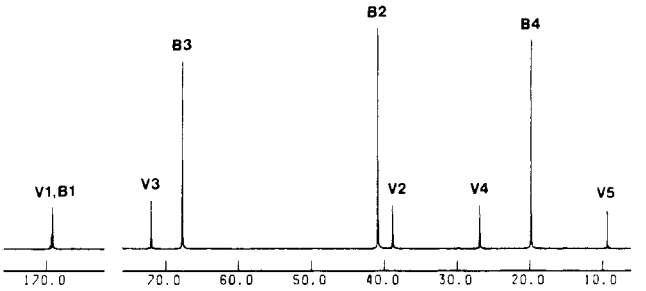

Figure 2. 62.9-MHz ^{13}C NMR spectrum of bacterial P(HB-*co*-20% HV) in $CDCl_3$ at 23 °C. B and V refer to β-hydroxybutyrate and β-hydroxyvalerate units, respectively; numbering scheme from Figure 1. Chemical shifts are in ppm from internal Me_4Si.

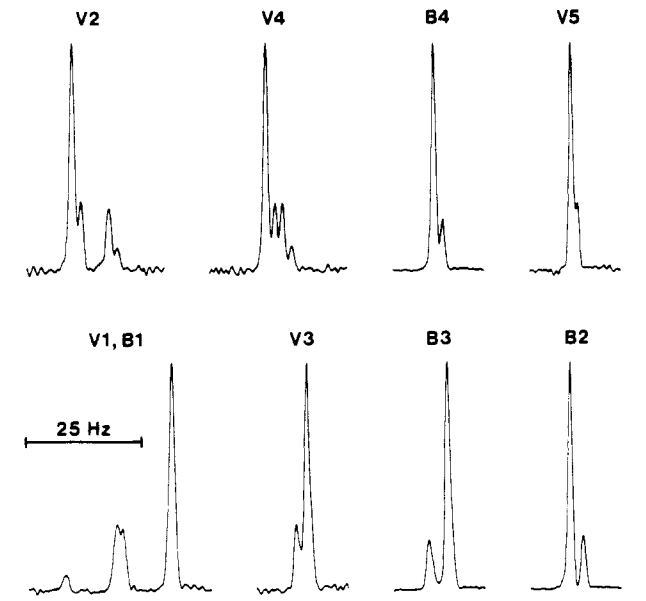

Figure 3. Expanded resolution-enhanced 62.9-MHz ^{13}C NMR spectra of P(HB-*co*-20% HV). Peak heights are not to scale. For numbering scheme see Figure 1.

X-ray Diffraction. X-ray diffraction measurements were made on a Philips powder diffractometer Model PW 1050/80 equipped with a graphite monochrometer and pulse height analyzer. Nickel-filtered Cu Kα radiation (λ = 0.1542 nm) was used. Crystallinities were measured for as-received powder samples and for films that had been cast from chloroform solution and allowed to stand for several weeks. The percentage of crystallinity was calculated from diffracted intensity data in the range 2θ = 6–40° by using Ruland's method as modified by Vonk.[10] The amorphous contribution to the X-ray scattering was estimated by computer fitting a series of linear functions connecting the diffraction peak minima. X-ray fiber diagrams were also recorded for all P(HB-*co*-HV) compositions with a Warhus camera. The films were calibrated with NaF.

Results and Discussion

Comonomer Sequence Distribution. The ^{13}C NMR spectrum of P(HB-*co*-20% HV) in $CDCl_3$ solution is shown in Figure 2. The indicated peak assignments are straightforward, with the chemical shifts for HB and HV units of the copolymer in close agreement with values previously reported[11] for the homopolymers PHB and PHV. As shown in Figure 3, each peak in the P(HB-*co*-HV) spectrum is split into multiplets due to comonomer sequence effects. The carbonyl region (V1, B1), for example, comprises four peaks, two singlets flanking a poorly resolved doublet; from left to right, these four peaks can be readily assigned[4,11] to VV, (VB, BV) and BB diad sequences (see Figure 4, where B and V refer to β-hydroxybutyrate and β-hydroxyvalerate units, respectively). Of the remaining resonances, most show a lower chemical shift sensitivity to the comonomer sequence. However, the main- and side-chain methylene carbon resonances of HV, V2 and V4, are split into four peaks. As shown in Figure 4, the V2 and V4 multiplets can be assigned to the V-centered triad sequences VVV, VVB, BVV, and BVB. Peak assignments for VVV and BVB triads are unequivocal, but those for VVB and BVV sequences are less certain. For the V2 multiplet it is assumed that the incremental chemical shift due to an asymmetric center three bonds removed is greater than that for one five bonds removed, and assignments are made accordingly. For V4, the VVB and BVV assignments are ambiguous. It should be noted, however, that the assignment of VVB and BVV triads (or VB and BV diads) is not critical to the statistical argument which follows.

Assuming the simplest model, a Bernoullian or random statistical process for HB/HV bacterial copolymerization, the diad fractions [VV], [VB], [BV], and [BB] can be calculated from F_V, the mole fraction of HV units in the polymer:[12]

$$[VV] = F_V^2 \quad (1)$$

$$[VB] = [BV] = F_V(1 - F_V) \quad (2)$$

$$[BB] = (1 - F_V)^2 \quad (3)$$

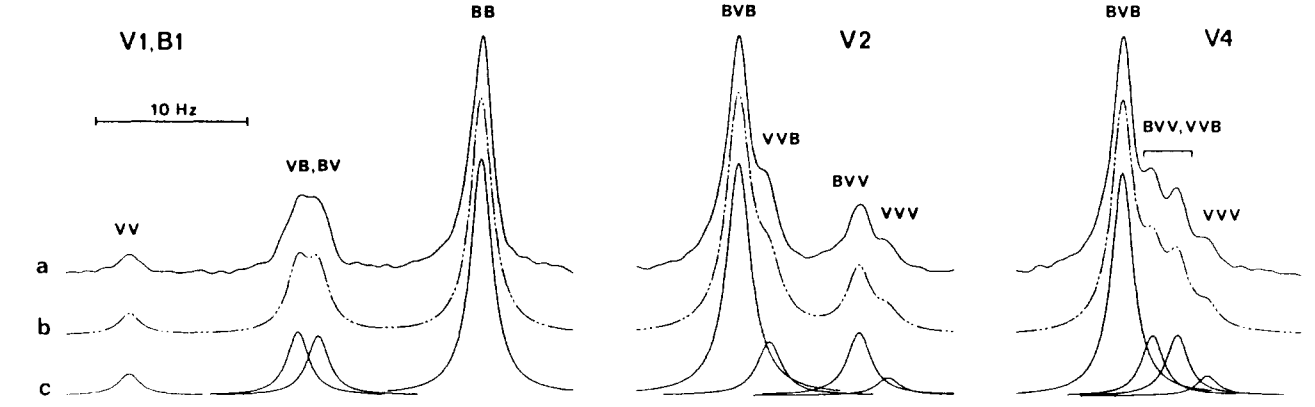

Figure 4. Experimental and calculated ^{13}C NMR spectra for the V1, B1, V2, and V4 resonances of P(HB-*co*-20% HV): (a) experimental spectrum; (b) LINESIM[8] curve-fit spectrum; (c) component Lorentzian peaks of curve-fit spectrum.

Table I
Experimental and Calculated Diad and V-Centered Triad Fractions (Relative Intensities) for P(HB-*co*-20% HV) and P(HB-*co*-47% HV) Samples from *Alcaligenes eutrophus*

			relative intensities			
			P(HB-*co*-20% HV)		P(HB-*co*-47% HV)	
carbon	chemical shift, ppm	sequence	obsd[a]	calcd[b]	obsd[a]	calcd[b]
B1, V1	169.12	BB	0.62 (0.64)	0.64	0.29 (0.28)	0.28
	169.29	BV[c]	0.17 } (0.31)	0.16	0.24 } (0.48)	0.25
	169.32	VB[c]	0.16 }	0.16	0.25 }	0.25
	169.49	VV	0.05 (0.05)	0.04	0.22 (0.24)	0.22
V2	38.88	BVB	0.63	0.64	0.30	0.28
	38.75	BVV	0.17	0.16	0.24	0.25
	38.85	VVB	0.15	0.16	0.23	0.25
	38.73	VVV	0.05	0.04	0.23	0.22
V4	26.91	BVB	0.61	0.64	0.29	0.28
	26.88	BVV[c]	0.17	0.16	0.24	0.25
	26.85	VVB[c]	0.17	0.16	0.22	0.25
	26.81	VVV	0.05	0.04	0.25	0.22

[a] Relative peak areas from LINESIM[8] curve fit; values in parentheses from integration. [b] Calculated values from eq 1–3. [c] Assignments uncertain; may be interchanged.

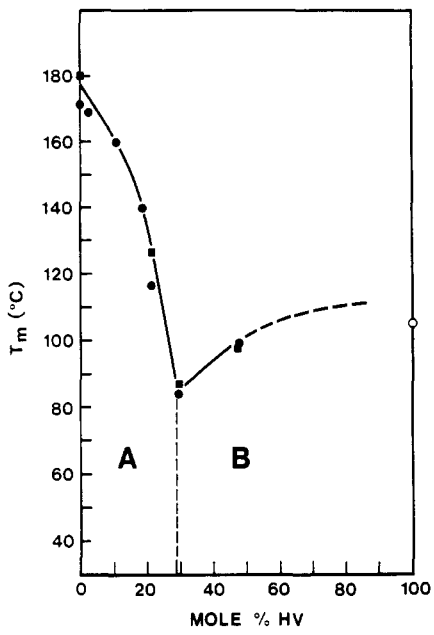

Figure 5. Melting point vs. composition curve for bacterial P(HB-*co*-HV). The open circle represents a racemic PHV sample. Closed circles were measured at 20 °C/min and the squares determined by extrapolation to zero heating rate. Samples with compositions in the region marked A produce X-ray diagrams showing only the PHB crystalline phase, and samples with compositions in the region marked B show only the PHV crystalline phase.

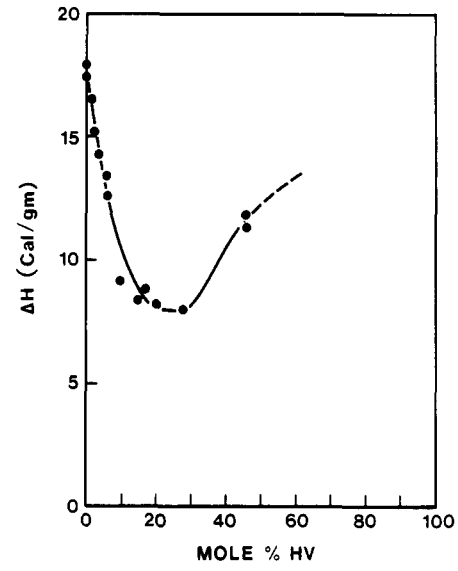

Figure 6. Enthalpy of fusion (ΔH) vs. composition curve for P(HB-*co*-HV).

If the sum of the V-centered triad fractions is normalized to one, rather than to F_V, then the triad fractions [VVV], [VVB], [BVV], and [BVB] are given by similar expressions; i.e., [VVV] = F_V^2, etc. Although all peaks in the P(HB-*co*-HV) spectrum could be fit to the Bernoullian model, the present analysis is confined to the carbonyl diads and the V2 and V4 V-centered triads. Table I lists the diad and normalized triad fractions calculated from F_V (determined by ^{1}H NMR spectroscopy)[6] for two representative P(HB-*co*-HV) samples containing 20 and 47 mol % HV, respectively. Also listed are the corresponding measured distributions. For the carbonyl resonances (V1, B1) the diad fractions were determined both by spectrometer integration and curve fitting; for V2 and V4, where peak overlap is severe, only the latter procedure was used. Curve-fitting results for P(HB-*co*-20% HV) are shown in Figure 4. Within the experimental uncertainty in the measured diad and triad fractions (±0.02–0.03) there is good agreement between the observed values and calculated distributions based on the Bernoullian model. Thus, it may be concluded that the comonomer distribution in P(HB/HV) copolymers produced by *Alcaligenes eutrophus* is statistically random.

Thermal Analysis. As shown in Figure 5, the melting point vs. composition curve for P(HB-*co*-HV) shows eutectic-like behavior. The melting point of pure PHB is 179 °C, while that of pure PHV, from the literature, is 105–108 °C.[13] However, the latter value corresponds to the melting point of a racemic polymer and is therefore lower than that expected for chiral PHV. For example, the melting point for racemic PHB has been reported to be 167–169 °C,[14] 10 °C lower than that of the chiral material. The melting point at the minimum of Figure 5 is approximately 84 °C.

Heats of fusion measured from the thermograms show a similar trend with the values of ΔH_u being lowest in the composition range near 30 mol % HV units (Figure 6). The type of behavior observed here is typical of statistically random copolymers where both monomers can crystallize and the monomer units of one type are included in the crystal lattice of the other and vice versa, i.e., the behavior of an isodimorphic system.[5]

In most copolymer systems where both homopolymers crystallize, a melting point minimum is not observed unless

Table II
X-ray Crystallinities of As-Received P(HB-*co*-HV) Powder Samples

mol % HV	% crystallinity	mol % HV	% crystallinity
0	64 ± 5	20	62 ± 5
2	64 ± 5	29	68 ± 5
10	61 ± 5	47	74 ± 5
18	66 ± 5		

there is a similarity in the crystalline conformations of each. For PHB and PHV this is indeed the case since both polymer chains crystallize as 2_1 helices with 0.596- and 0.556-nm fiber repeats, respectively.[2,13-15]

The observed melting points of the copolyesters with compositions containing less than 30 mol % HV can be predicted by using the Flory equation for melting point depression[16]

$$1/T_m - 1/T_m^\circ = -R \ln (X_B)/\Delta H_u \quad (4)$$

where ΔH_u is the enthalpy of fusion per mole of repeating units, R is the universal gas constant in appropriate units, T_m is the melting point of the copolymer, T_m° is the melting point of the homopolymer (PHB), and X_B is the mole fraction of HB units in the copolymer. The value of ΔH_u derived from the classical Flory plot of $1/T_m$ vs. $-\ln (X_B)$ was 1592 cal mol^{-1}. This value was significantly smaller than ΔH_u observed for pure PHB from a DSC measurement (2797 cal mol^{-1}) after correction for the degree of crystallinity (from X-ray measurements). Higher values of ΔH_u than those derived from the Flory plot are quite common.

Measured melting points and heats of fusion for as-received powders and annealed samples were practically identical. These observations indicate that the copolymers readily crystallize during precipitation with methanol from chloroform solution since this was the process used to prepare the as-received samples.[4] This behavior was first reported by Lundgren et al.,[17] who considered the lamellar appearance of the precipitate in electron micrographs to be diagnostic for PHB. However, melt- and solution-cast films (especially of P(HB/HV) copolyesters) tend to crystallize much more slowly and may require several weeks to reach equilibrium crystallinity.[6,18]

X-ray Diffraction Analysis. X-ray diffraction traces recorded for P(HB-*co*-HV) films cast from chloroform solution showed the presence of only one crystalline phase at all compositions between 0 and 47 mol % HV. The phase present at compositions up to the melting point minimum was that of pure PHB (fiber repeat, 0.596 nm),[14,15] while after the minimum, all observed X-ray diffraction lines could be accounted for by invoking the PHV lattice (fiber repeat, 0.556 nm).[2,13] At no composition studied were X-ray reflections due to mixed crystalline forms of PHB and PHV observed (Figure 7). X-ray measurements of the degree of crystallinity gave highly reproducible values ranging from 61 to 74% (Table II). It is important to note that the crystallinity measurements were made on samples which had been aged for at least several weeks. This was necessary because the rate of crystallization is variable and extremely slow in these copolyesters. If the measurements are made before equilibrium crystallization is reached, the degree of crystallinity may appear to be composition dependent, as has recently been reported elsewhere.[19] These observations along with the knowledge that the comonomer sequence distribution in P(HB-*co*-HV) is statistically random are in keeping with the hypothesis of isodimorphism.

Measurements of d spacings from X-ray diffraction diagrams indicate an expansion of the (110) plane of the PHB lattice as the HV content of the polymer increases (Figure 8). Figure 8 also shows that the (020) and (002) d spacings are invariant, leading to the conclusion that only the a parameter of the unit cell is changing. The calculated linear increase in a runs from 0.576 nm for PHB to 0.605 nm for P(HB-*co*-29% HV). Thus, for HV contents up to 29 mol %, HV units are accomodated in the PHB crystal lattice by a small lateral expansion of the unit cell, while the fiber repeat remains unchanged.

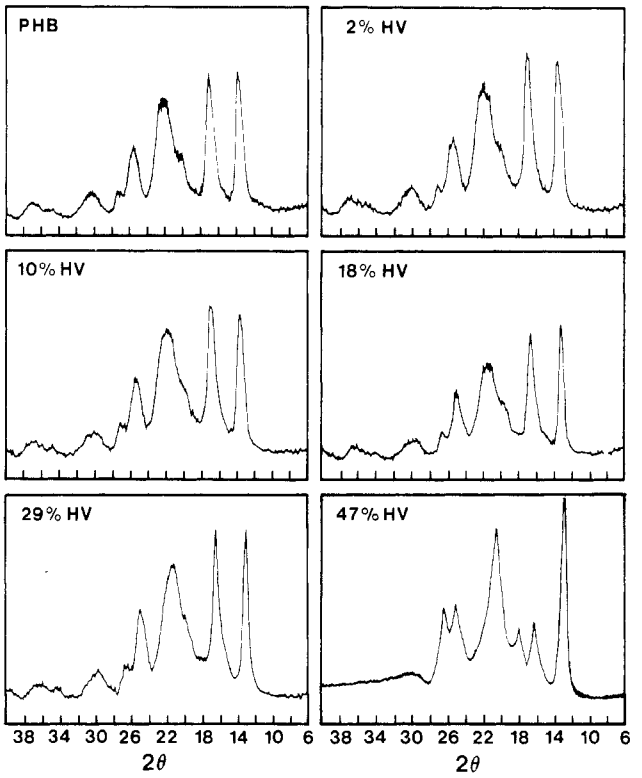

Figure 7. X-ray powder diffraction traces of as-received PHB and P(HB-*co*-HV) with increasing HV contents. Samples with HV contents between 0 and 29 mol % crystallize in the PHB lattice, while P(HB-*co*-47% HV) crystallizes in the PHV lattice.

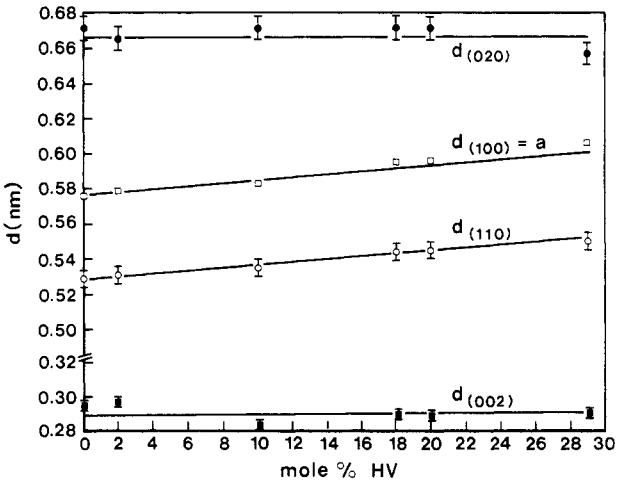

Figure 8. X-ray diffraction d spacings of the (110), (020), and (002) reflections measured from fiber diagrams for the PHB lattice as a function of P(HB-*co*-HV) composition. Also shown is the a lattice parameter calculated from the (110) d spacing.

^{13}C CP/MAS NMR Spectroscopy. The techniques of ^{13}C CP/MAS NMR spectroscopy yield moderately high resolution spectra in the solid state.[20] The chemical shifts obtained from these spectra represent the isotropic values for the solid state. Although ^{13}C CP/MAS NMR yields isotropic shifts as in solution, the solid-state spectra can

Table III
^{13}C CP/MAS NMR Chemical Shifts for P(HB-co-HV)

carbon[a]	^{13}C chemical shift,[b] ppm	
	HB unit	HV unit
C=O (B1, V1)	170.6 (0.4)	170.6 (0.4)
CH (B3, V3)	69.6 (0.4)	71.4 (0.3)
CH_2 (B2, V2)	43.9 (0.4)	41.6 (0.3)
CH_2 (V4)		29.5 (0.3)
CH_3 (B4, V5)	21.9 (0.5)	11.1 (0.3)

[a] Carbon numbering scheme from Figure 1. [b] Chemical shifts are average values for well-ordered carbon sites in all samples (films and powders). The values in parentheses are standard deviations of the observed shifts from the average.

be more complex due to inequivalences that may be induced between chemically equivalent nuclei by solid-state effects. The interpretation of these complex spectra, especially in conjunction with X-ray diffraction data, has yielded much information on the crystalline structure of both natural and synthetic polymers, as shown by recent work on cellulose,[21] starch,[22] and polypropylene.[23]

The line widths in ^{13}C CP/MAS spectra are dependent on the short-range order about the carbon atom whose resonance is observed. In general the sharpest resonances (i.e., a narrow distribution of chemical shifts) will be observed for carbon atoms in highly ordered environments. Carbon atoms in poorly ordered environments, amorphous or imperfect crystalline regions, will have a wider distribution of chemical shifts and give rise to broad resonances.

Solid-state ^{13}C NMR spectra of a series of P(HB-co-HV) film samples of increasing HV content are shown in Figure 9. The assignments for resonances due to HB and HV monomer units are listed in Table III.

For comonomer compositions up to 30 mol % HV (i.e., up to the melting point minimum) the HV methyl resonance is broad, indicating that these carbon atoms are in a poorly ordered environment. Above 30 mol % HV a sharp resonance is superimposed on the broad one, indicating that some HV methyl carbon atoms are now in a well-ordered environment. Similar behavior is observed for the HV side-chain methylene carbon resonance. With increasing HV content the backbone methylene and methine carbon resonances of the HV monomer units increase in intensity, as expected. Resonances from these carbons in both monomer units are relatively sharp, indicating that the disorder of the HV repeating units below the composition at the melting point minimum is mainly in the ethyl side chain, not the polymer backbone.

In the solid-state ^{13}C NMR spectrum of P(HB-co-HV) containing 47 mol % HV (the only sample studied that crystallizes in the PHV lattice) each carbon in the HV repeating unit gives rise to both broad and sharp resonances. Thus, there are HV repeating units that are well-ordered and some that are much less so. In addition, there is a definite chemical shift difference between carbon atoms in these two environments; this suggests that the two environments must be considerably different. In contrast, all carbons in the HB repeating unit show sharp resonances which occur at the same chemical shifts observed for copolyesters that crystallize in the PHB lattice (cf. P(HB-co-29% HV) in Figure 9). Thus, the HB carbons must be in very similar environments in both lattices. The only exception is the HB methyl side-chain carbon of P(HB-co-47% HV), which gives rise to both broad and narrow resonances. This indicates that some, but not all, of the HB methyl groups are poorly ordered in the PHV lattice.

In summary, it appears that the transformation from the PHB lattice to the PHV lattice results in little change of the well-ordered environment of the HB repeating units, with the exception that some of the HB methyl groups become less ordered in the PHV lattice. For compositions below 30 mol % HV, the HV repeating units are poorly ordered in the PHB lattice. Above the lattice-transition point some HV units become well-ordered in a different environment in the PHV lattice while the rest remain disordered.

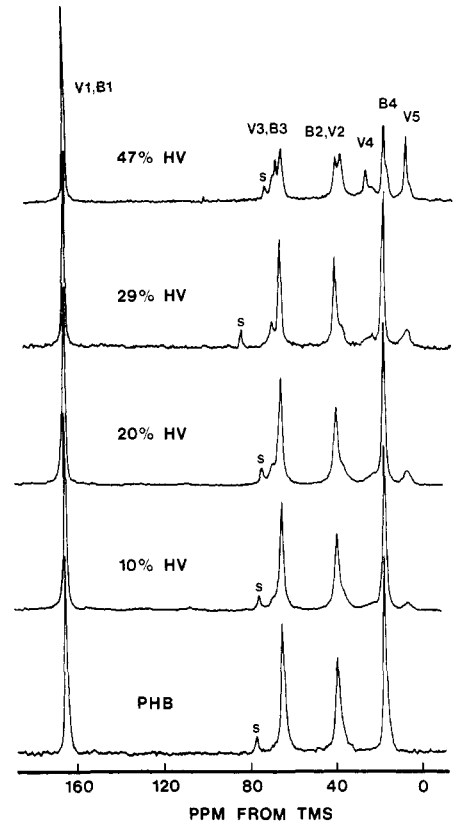

Figure 9. 22.6-MHz ^{13}C CP/MAS NMR spectra of P(HB-co-HV) solution-cast films with increasing HV content. All spectra are the accumulation of ~20 000 scans, except for the P(HB-co-47% HV) spectrum, which is the accumulation of 40 000 scans. Peaks marked s are due to spinning sidebands; numbering scheme from Figure 1.

Figure 10 shows ^{13}C CP/MAS spectra of P(HB-co-47% HV) after different sample treatments and of P(HB-co-29% HV), which is included for reference. From a comparison of spectra of the 47 mol % HV copolyester as a powder and as a film, it is apparent that the resonances of the two monomer units show opposite behaviors. The film has a higher ratio of the less-ordered to well-ordered resonances for HV repeating units, while the less-ordered resonance of the HB methyl carbon nearly disappears. When the film is stretched, this trend continues; the ratio of the less-ordered resonances for HV repeating units increases further, and the less-ordered resonance of the HB methyl carbon totally disappears. On annealing, the behavior of the comonomers is reversed; the broad resonance due to the HB methyl carbon reappears, while the broad resonances for the HV ethyl group carbons disappear. The sharp resonances for the other HV carbons increase at the expense of the broad resonances.

Conclusions

All physical evidence obtained in this study supports the isodimorphism hypothesis. As stated by Allegra,[5] the requirements for isomorphism (which also apply to isodimorphism in a more specific sense) are (a) that the two different monomer units must have approximately the

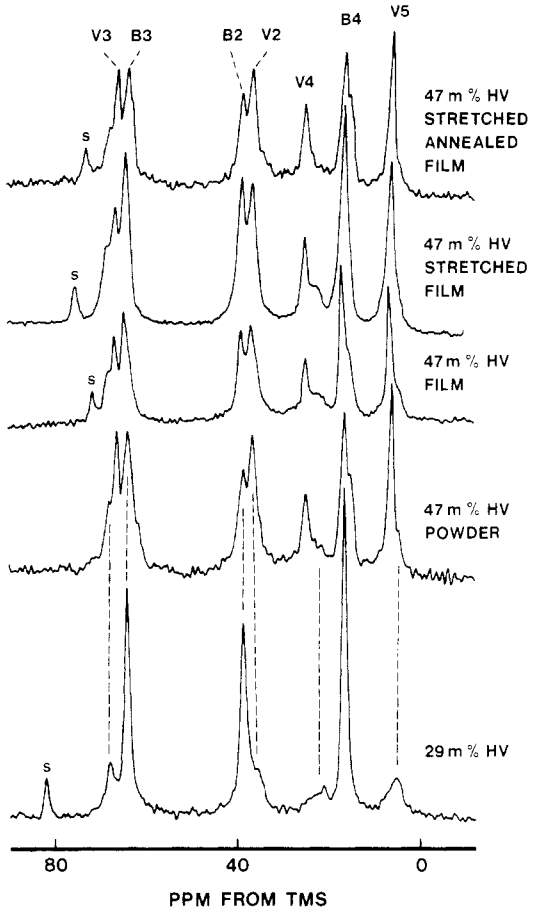

Figure 10. 22.6-MHz ^{13}C CP/MAS NMR spectra of solid P(HB-*co*-HV). The carbonyl resonance is not shown in this expansion. The spectra of P(HB-*co*-29% HV) and the P(HB-*co*-47% HV) powder sample are the accumulation of 20 000 scans; the rest are the accumulation of 40 000 scans. Peaks marked s are due to spinning sidebands; numbering scheme from Figure 1.

same shape and occupy the same volume and (b) that the chain conformation of both homopolymers must be compatible with either crystal lattice. Thus, copolymers are *isomorphic* when *one* crystalline phase containing both monomer types is detected at all compositions; in the ideal case a melting point minimum is not observed. Copolymers are *isodimorphic* when *two* crystalline phases containing both monomer types are detected. Each phase is found at compositions on opposite sides of a melting point minimum. This is the case for the P(HB-*co*-HV) system, and it results from the fact that the crystalline structures of PHB and PHV have remarkably similar chain conformations; i.e., both exist as 2_1 helices with advances per monomer unit of 0.298 and 0.278 nm, respectively.[2,13-15] From unit cell data, the volumes of the two monomer units are 0.11 nm^3 (PHB) and 0.13 nm^3 (PHV). We have also argued above that small changes in the *d* spacings for the (110) plane of PHB do not constitute a significant change in the lattice. The P(HB-*co*-HV) system is remarkable for its high crystallinity throughout the 0–47 mol % HV composition range, a fact consistent with isodimorphic behavior and in keeping with the observation of a minimum in the melting point curve.

While the Flory copolymer equation can be empirically modified to predict melting points for a system such as P(HB-*co*-HV), there is clearly a theoretical deficiency in this area. A recent attempt to cover this deficiency[24] relates to the case where "the crystallizable units are miscible in the melt but immiscible in the crystalline phase". This description fails to account for isodimorphism. Aside from the scientific interest of an isodimorphic system, there is an important technical advantage in being able to maintain crystallinity while the melting point changes over a range of almost 100 °C. Most copolymer systems where both homopolymers crystallize become amorphous over the entire middle range of compositions. This is due to incompatibility of the crystal lattices. In the present case, the comonomers are clearly chemically and geometrically similar, yet there is a large decrease in the enthalpy of fusion at intermediate copolymer compositions. The decrease in the melting point is almost entirely due to the ΔH_u term of the classical equation relating melting point, ΔH_u, and ΔS_u. This suggests that the crystal packing is disturbed by the inclusion of HV units in the PHB lattice and vice versa.

Acknowledgment. We thank Steven Bloembergen for performing DSC analyses and for many helpful discussions.

References and Notes

(1) Holmes, P. A. *Phys. Technol.* **1985**, *16*, 32.
(2) Marchessault, R. H.; Morikawa, H.; Revol, J.-F.; Bluhm, T. L. *Macromolecules* **1984**, *17*, 1882.
(3) Wallen, L. L.; Rohwedder, W. K. *Environ. Sci. Technol.* **1974**, *8*, 576.
(4) Holmes, P. A.; Wright, L. F.; Collins, S. H. Eur. Pat. Appl. 0 052 459, 1982. Eur. Pat. Appl. 0 069 497, 1983.
(5) Allegra, G.; Bassi, I. W. *Adv. Polym. Sci.* **1969**, *6*, 549.
(6) Bloembergen, S.; Holden, D. A.; Hamer, G. K.; Bluhm, T. L.; Marchessault, R. H. *Macromolecules*, preceding paper in this issue.
(7) Ferrige, A. G.; Lindon, J. C. *J. Magn. Reson.* **1978**, *31*, 337.
(8) Barron, P. Bruker ABACUS Program ABA051; Spectrospin AG; Fällanden, Switzerland, 1985.
(9) Alemany, L. B.; Grant, D. M.; Pugmire, R. J.; Alger, T. D.; Zilm, K. W. *J. Am. Chem. Soc.* **1983**, *105*, 2133.
(10) Vonk, C. G. *J. Appl. Crystallogr.* **1973**, *6*, 148.
(11) (a) Iida, M.; Hayase, S.; Araki, T. *Macromolecules* **1978**, *11*, 490. (b) Doi, Y.; Kunioka, M.; Nakamura, Y.; Soga, K. *Macromolecules* **1986**, *19*, 1274.
(12) Randall, J. C. *Polymer Sequence Determination*; Academic: New York, 1977; Chapter 4.
(13) Yokouchi, M.; Chatani, Y.; Tadokoro, H.; Tani, H. *Polym. J. (Tokyo)* **1974**, *6*, 248.
(14) (a) Yokouchi, M.; Chatani, Y.; Tadokoro, H.; Teranishi, K.; Tani, H. *Polymer* **1973**, *14*, 267. (b) Agostini, D. E.; Lando, J. B.; Shelton, J. R. *J. Polym. Sci., Polym. Chem. Ed.* **1971**, *9*, 2775. (c) Shelton, J. R.; Agostini, D. E.; Lando, J. B. *J. Polym. Sci., Polym. Chem. Ed.* **1971**, *9*, 2789.
(15) Cornibert, J.; Marchessault, R. H. *J. Mol. Biol.* **1972**, *71*, 735.
(16) (a) Flory, P. J. *J. Chem. Phys.* **1949**, *17*, 223. (b) Flory, P. J. *Trans. Faraday Soc.* **1955**, *51*, 848.
(17) Lundgren, D. G.; Alper, R.; Schnaitman, C.; Marchessault, R. H. *J. Bacteriol.* **1965**, *89*, 245.
(18) Barham, P. J.; Keller, A.; Otun, E. L.; Holmes, P. A. *J. Mater. Sci.* **1984**, *19*, 2781.
(19) Owen, A. J. *Colloid Polym. Sci.* **1985**, *263*, 799.
(20) (a) Schaefer, J.; Stejskal, E. O. In *Topics in Carbon-13 NMR Spectroscopy*; Wiley: New York, 1979; Vol. 3. (b) Lyerla, J. R. *Contemp. Top. Polym. Sci.* **1979**, *3*, 143. (c) Wasylishen, R. E.; Fyfe, C. A. *Annu. Rep. NMR Spectrosc.* **1982**, *12*, 1. (d) Fyfe, C. A.; Dudley, R. L.; Stephenson, P. J.; Deslandes, Y.; Hamer, G. K.; Marchessault, R. H. *J. Macromol. Sci., Rev. Macromol. Chem. Phys.* **1983**, *C23*, 187. (e) Fyfe, C. A. *Solid State NMR for Chemists*; CFC: Guelph, Canada, 1984.
(21) Horii, R.; Hirai, A.; Kitamaru, R. *Polym. Bull. (Berlin)* **1982**, *8*, 163.
(22) (a) Veregin, R. P.; Fyfe, C. A.; Marchessault, R. H.; Taylor, M. G. *Macromolecules* **1986**, *19*, 1030. (b) Gidley, M. J.; Bociek, S. M. *J. Am. Chem. Soc.* **1985**, *107*, 7040.
(23) (a) Bunn, A.; Cudby, M. E. A.; Harris, R. K.; Packer, K. J.; Say, B. J. *J. Chem. Soc., Chem. Commun.* **1981**, 15. (b) Bunn, A.; Cudby, M. E. A.; Harris, R. K.; Packer, K. J.; Say, B. J. *Polymer* **1982**, *23*, 694.
(24) Theil, M. H. *Polym. Prepr. (Am. Chem. Soc., Div. Polym. Chem.)* **1983**, *24*(2), 109.